Random Phase Modulation in Load Modulated Arrays

Sandeep Bhat and A. Chockalingam
Department of ECE, Indian Institute of Science, Bangalore 560012

***Abstract*—Load modulated arrays (LMAs) are gaining research attention as an attractive transmitter architecture for multiple-input multiple-output (MIMO) systems. A key advantage of LMAs is that they eliminate the need for RF chains at the transmitter (consisting of DACs, mixers, filters) and use only one central power amplifier for any number of antenna elements. The algorithmic complexity of the construction of high spectral efficiency load modulation (LM) signal sets for large arrays that attempts to maximize the angular separation between load impedance vectors is high. In this paper, we propose high spectral efficiency LM signal sets for large arrays. In particular, we propose *random phase modulation* (RPM) for LMAs, where randomly chosen phase vectors constitute the LM signal set. The LM signal sets generated using RPM are shown to achieve performance close to within a fraction of a dB compared to the performance achieved by algorithmically constructed LM signal sets, particularly when the signal set size and signal dimension are large. Further, we propose the use of *random phase precoding* (RPP) and *precoder index modulation* (PIM) in LMAs, which is shown to achieve a performance improvement of about 7-8 dB at 10^{-4} bit error rate.**

Keywords: *Load modulation, load modulated array, multidimensional hypersphere, random phase modulation., precoder index modulation.*

I. Introduction

Multiple-input multiple-output (MIMO) systems are poised to become a mainstay in future wireless networks. Multiple antennas are used at the transmitter and receiver terminals to exploit independent spatial dimensions (thus achieving a diversity gain) and obtain an increased received signal power by coherent combining (thus achieving a power gain). [1],[2]. Systems employing large number of antennas to realize substantial diversity and power gains are getting popular [3],[4]. MIMO transmitters typically use a separate radio frequency (RF) chain (consisting of DACs, mixers, filters) and a power amplifier (PA) for each antenna element. This leads to an increase in the size and cost of MIMO transmitters with increasing number of antennas. Also, rectangular QAM constellations and OFDM techniques impose linearity requirements on the PAs that affect power efficiency. In the wake of increased energy consumption by the Information and Communication Technology (ICT) sector [5], developing energy efficient array architectures has become an important goal in next generation wireless systems. Load modulated arrays (LMA) [6],[7] is emerging as a promising MIMO array architecture that alleviates the aforementioned issues.

In load modulated MIMO transmitters, all antennas are driven by a sinusoid of fixed amplitude and phase and a single central power amplifier (CPA). The antenna load impedances are tuned (modulated) according to the information bearing signal, giving the scheme the name 'load modulation' (LM), as opposed to conventional voltage modulation. The signaling constellation is essentially implemented in the analog domain, doing away with the need for DACs and mixers in the process and the CPA constantly operates at its peak power.

Since the effective load impedance in LMAs varies according to the information signal, there may be a mismatch with the circuit impedance and power may be reflected back to the CPA, resulting in reduced efficiency. In order to prevent this mismatch, all possible transmit signals (LM signal set) are chosen to be on the surface of a multidimensional hypersphere. This ensures that the sum power for all the transmit signals is the same and hence improves the CPA efficiency. The constant radius nature of this modulation scheme allows it to be broadly termed as phase shift keying on the hypersphere [8] or phase modulation on the hypersphere [9]. However, constructing such a LM signal set that achieves good performance requires solving optimization problems which quickly scale up in complexity as the size of the signal set increases. For example, the algorithmic complexity of the construction of high spectral efficiency LM signal sets for large arrays that attempts to maximize the angular separation between load impedance vectors (e.g., using k-means clustering [9]-[11]) is high.

In this regard, our new contributions in this paper can be summarized as follows. First, we propose random phase modulation (RPM) for LMAs, where randomly chosen phase vectors constitute the LM signal set, which can be easily generated for high spectral efficiency large-dimension LMAs. In addition to its low-complexity advantage, RPM in LMAs achieves good performance as well. For example, simulation results show that the LM signal sets generated using RPM achieve performance close to within a fraction of a dB compared to the performance achieved by the LM signal sets constructed by k-means clustering (kMC) algorithm, particularly when the signal set size (which determines the achieved rate in bits per channel use (bpcu)), and the signal

This work was supported in part by the J. C. Bose National Fellowship, Department of Science and Technology, Government of India.

dimension (number of transmit antennas) are large. For example, in a 16×16 load modulated MIMO system with 8 bpcu, the performance difference between RPM and kMC signal sets is only about 0.3 dB at 10^{-4} bit error rate (BER). Second, we propose the use of random phase precoding (RPP) and precoder index modulation (PIM) in LMAs. The use of RPP and PIM is shown to result in a performance improvement of about 7-8 dB at 10^{-4} BER. This performance improvement is because of the time diversity gains possible in RPP and the possibility of using a smaller-sized LM signal set in PIM to achieve a certain rate in bpcu.

The rest of this paper is organized as follows. LMAs are introduced in Section II. The proposed RPM scheme for LMAs and its performance are presented in Section III. RPP and PIM schemes for LMAs and their performance are presented in Section IV. Conclusions are presented in Section V.

II. Load modulated arrays

A. Voltage modulation vs load modulation

Conventional RF transmitter hardware uses 'voltage modulation', where the circuit impedance is kept fixed and a voltage is formed proportional to the information bearing signal. Voltage modulation is advantageous because the circuit impedance can be matched to the antenna load impedance, leading to optimum power transfer. However, a drawback is that the PA needs to be considerably backed-off to guarantee linear response over the full input voltage range. In traditional multi-antenna transmitters, multiple PAs (one PA per antenna) must be driven at high backoffs. Power efficiency and RF hardware cost, therefore, become concerns when the traditional voltage modulation is employed in large antenna arrays. On the contrary, in 'load modulation', the voltage is held constant (single frequency sinusoid of fixed magnitude and phase) and the antenna load impedance is tuned by the information bearing signal [6].

B. LMAs

Load modulation is attractive for large antenna arrays [7]. LMA refers to an array architecture (see Fig. 1) in which the multiple antenna load impedances are tuned by the information bearing signals while being driven by a constant amplitude sinusoid and a single central PA (see the $v_0\cos\omega t$ source and the CPA in Fig. 1) [6]-[9]. Figure 1 shows an LMA with n_t transmit antennas. The load impedance in the lth antenna, denoted by $Z_l(t)$, is chosen to be proportional to the lth transmit signal $s_l(t)$, $l=1,2,\cdots,n_t$. The circuit that achieves this is referred to as a 'load modulator'. A load modulator can be implemented using varactor diodes or pin-diodes, where input currents to antenna loads are generated based on information bearing signals. The effective admittance

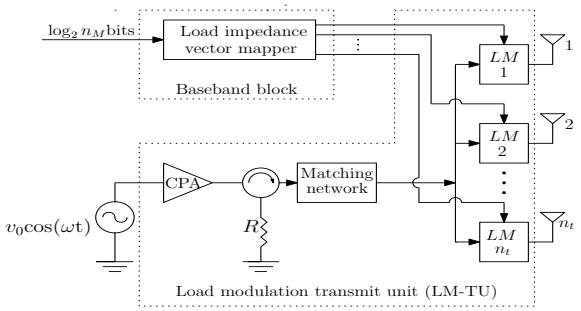

Fig. 1. Load modulated array.

seen by the power source is the sum of the admittances of all antenna loads, i.e.,

$$Y(t)=\sum_{l=1}^{n_t}\frac{1}{Z_l(t)}. \tag{1}$$

The single power source becomes equivalent to n_t parallel power sources, each with an average admittance $Y(t)/n_t$. Since $Y(t)$ varies with the information signals, mismatch between circuit impedance and effective antenna impedance may arise, and this can cause power to be reflected back to the CPA. So a circulator is used to redirect any reflected power to a resistor R. In Fig. 1, the assembly of the CPA, circulator, n_t antennas, and their associated load modulators is referred to as a 'load modulation transmit unit' (LM-TU).

For large arrays (large n_t), because of the law of large numbers, the average admittance $Y(t)/n_t$ does not vary much even if the individual admittances may vary significantly. This, in turn, results in only a small power being reflected back to the CPA in large arrays. The CPA efficiency is determined by the peak to average sum power ratio (PASPR), which is the peak to average power ratio (PAPR) aggregated over all the antenna elements [9]. For large arrays, the PASPR tends to one asymptotically due to law of large numbers. Therefore, with large arrays, the CPA can be operated at its peak power. For small arrays (small n_t), however, the PASPR can be more than one. To obtain a PASPR close to one in small arrays, it is desired that the sum power radiated by the antennas be made constant. A way to achieve this is to use phase modulation on the hypersphere (PMH) [9].

C. Phase modulation on the hypersphere

PMH uses points on the n_t-dimensional hypersphere to form the LM signal set. Let $\mathbb{S}_{\text{LM}}$ denote the n_M-ary LM signal set, where $n_M\triangleq|\mathbb{S}_{\text{LM}}|$. Let

$$\mathbb{S}_{\text{H}}(n_t,P)=\{\mathbf{s}\in\mathbb{C}^{n_t}\mid\|\mathbf{s}\|^2=P\} \tag{2}$$

denote the n_t-dimensional complex-valued hypersphere of radius $\sqrt{P}$. Then,

$$\mathbb{S}_{\text{LM}}=\{\mathbf{s}_1,\mathbf{s}_2,\cdots,\mathbf{s}_{n_M}\}\subset\mathbb{S}_{\text{H}}(n_t,P). \tag{3}$$

One way to obtain the signal vectors that constitute $\mathbb{S}_{\text{LM}}$ is by generating uniformly distributed vectors on the hypersphere and clustering them [11]. An $n_t \times 1$ signal vector $\mathbf{s}$ from $\mathbb{S}_{\text{LM}}$ chosen based on $\log_2 n_M$ information bits gets sent in a channel use by the n_t load modulators as shown in Fig. 1.

LM signal detection: Assuming n_r antennas at the receiver, the received signal vector $\mathbf{y}$ can be written as

$$\mathbf{y} = \mathbf{H}\mathbf{s} + \mathbf{n}, \tag{4}$$

where $\mathbf{H}$ denotes the $n_r \times n_t$ matrix of channel gains such that the gain from the jth transmit antenna to the ith receive antenna $h_{ij} \sim \mathcal{CN}(0,1)$ and $\mathbf{n}$ is the $n_r \times 1$ noise vector with $\mathbf{n} \sim \mathcal{CN}(0, \sigma^2\mathbf{I})$. The maximum-likelihood (ML) detection rule is then given by

$$\hat{\mathbf{s}} = \underset{\mathbf{s}\in\mathbb{S}_{\text{LM}}}{\operatorname{argmin}} \|\mathbf{y} - \mathbf{H}\mathbf{s}\|^2. \tag{5}$$

III. Proposed RPM for LMAs

Optimal construction of the LM signal set $\mathbb{S}_{\text{LM}}$ defined in the previous section can be formulated as a spherical code construction problem [9]. A spherical code $C(K, 2M, \theta_{min})$ is defined as K code vectors in $\mathbb{R}^{2M}$ with a least angular separation θ_{min}. For example, $C(n_M, 2n_t, \theta_{min})$ could be thought of as the optimal signal set for an LMA with n_t transmit antennas and achieving a spectral efficiency of $\log_2 n_M$ bpcu. However, such spherical codes are known only for some M and K [10]. Suboptimal methods may therefore be used to construct LM signal sets. One method is to use spherical k-means clustering algorithm to solve the optimization problem [11]. This algorithm operates on a large number of vectors on a multidimensional hypersphere and iterates to group them into k clusters while maximizing the inter-cluster distances. To construct an LM signal set using the spherical k-means clustering algorithm, a large number of vectors are generated uniformly on the surface of a $2n_t$-dimensional hypersphere and grouped into n_M clusters. When the number of dimensions (n_t) is large and the vectors do not possess a inherent cluster structure, this algorithm can get expensive in terms of complexity when the required number of clusters (n_M) increases.

A. Proposed RPM-LM

As opposed to the algorithmic construction approach whose complexity can be high, here we propose to use randomly chosen vectors on the surface of a multidimensional hypersphere as the LM signal set. Because the antenna loads are modulated by this random choice of phase vectors, we term this scheme as 'random phase modulation LM' (RPM-LM). The RPM-LM signal set $\mathbb{S}_{\text{RPM-LM}}$ is constructed as follows.

- Generate $\mathbf{v}_i \sim \mathcal{CN}(0, \mathbf{I}_{n_t}), i = 1, 2, \cdots, n_M$.
- Compute $\mathbf{s}_i = \frac{\mathbf{v}_i}{\|\mathbf{v}_i\|_2}$, $i = 1, 2, \cdots, n_M$.
- $\mathbb{S}_{\text{RPM-LM}} \triangleq \{\mathbf{s}_1, \mathbf{s}_2, \cdots, \mathbf{s}_{n_M}\}$.

RPM-LM has the advantage of easy generation of the signal set. We will see that RPM-LM signal sets can achieve performance close to that of signal sets constructed by k-means clustering algorithm, particularly when the dimensionality (n_t) and size of the signal set (n_M) are high.

B. Upper bound on average BER

With the ML detection in (5), the conditional pairwise error probability (PEP) of $\mathbf{s}$ being decoded as $\tilde{\mathbf{s}}$ can be written as

$$P(\mathbf{s} \to \tilde{\mathbf{s}}|\mathbf{H}) = P(\|\mathbf{y} - \mathbf{H}\mathbf{s}\|^2 > \|\mathbf{y} - \mathbf{H}\tilde{\mathbf{s}}\|^2). \tag{6}$$

Substituting (4) in (6), we get

$$\begin{aligned} P(\mathbf{s} \to \tilde{\mathbf{s}}|\mathbf{H}) &= P(\|\mathbf{n}\|^2 > \|\mathbf{H}(\mathbf{s} - \tilde{\mathbf{s}})\|^2|\mathbf{H}) \\ &= P\big(2\Re\big(\mathbf{n}^\dagger\mathbf{H}(\mathbf{s} - \tilde{\mathbf{s}})\big) > \|\mathbf{H}(\mathbf{s} - \tilde{\mathbf{s}})\|^2\big), \end{aligned} \tag{7}$$

where $\Re(\cdot)$ denotes real part, $(\cdot)^\dagger$ denotes conjugate transpose, and $2\Re\big(\mathbf{n}^\dagger\mathbf{H}(\mathbf{s} - \tilde{\mathbf{s}})\big)$ is a Gaussian random variable with zero mean and variance $2\sigma^2\|\mathbf{H}(\mathbf{s} - \tilde{\mathbf{s}})\|^2$. Therefore,

$$P(\mathbf{s} \to \tilde{\mathbf{s}}|\mathbf{H}) = Q\big(\sqrt{|\mathbf{H}(\mathbf{s} - \tilde{\mathbf{s}})\|^2/2\sigma^2}\big), \tag{8}$$

where $Q(x) = \frac{1}{\sqrt{2\pi}}\int_x^\infty e^{-\frac{t^2}{2}}dt$. The computation of the unconditional PEP, $P(\mathbf{s} \to \tilde{\mathbf{s}})$, requires the expectation of $Q(\cdot)$ in (8) w.r.t. $\mathbf{H}$, which can be obtained as follows [12]:

$$\begin{aligned} P(\mathbf{s} \to \tilde{\mathbf{s}}) &= \mathbb{E}_{\mathbf{H}}\{P(\mathbf{s} \to \tilde{\mathbf{s}}|\mathbf{H})\} \\ &= \mathbb{E}_{\mathbf{H}}\big\{Q\big(\sqrt{|\mathbf{H}(\mathbf{s} - \tilde{\mathbf{s}})\|^2/2\sigma^2}\big)\big\} \\ &= f(\beta)^{n_r}\sum_{i=0}^{n_r-1}\binom{n_r - 1 + i}{i}(1 - f(\beta))^i, \end{aligned} \tag{9}$$

where $f(\beta) \triangleq \frac{1}{2}\Big(1 - \sqrt{\frac{\beta}{1+\beta}}\Big)$, and $\beta \triangleq \frac{\|\mathbf{s}-\tilde{\mathbf{s}}\|^2}{4\sigma^2}$. Now, an upper bound on the average BER based on union bounding can be obtained as

$$P_B \leq \frac{1}{n_M}\sum_{\mathbf{s}}\sum_{\tilde{\mathbf{s}}\neq\mathbf{s}} P(\mathbf{s} \to \tilde{\mathbf{s}})\frac{\delta(\mathbf{s}, \tilde{\mathbf{s}})}{\log_2 n_M}, \tag{10}$$

where $\delta(\mathbf{s}, \tilde{\mathbf{s}})$ is number of bits in which $\mathbf{s}$ differs from $\tilde{\mathbf{s}}$.

C. BER performance results

In this subsection, we present analytical and simulation results on the BER performance of RPM-LM. For comparison purposes, we also present the performance of the signal set generated by k-means clustering (kMC) algorithm; we refer to this scheme as the kMC-LM scheme. Figure 2 shows the performance of RPM-LM and kMC-LM in a MIMO system with $n_t = n_r = 8$, $n_M = 256$ (i.e., 8 bpcu), and ML detection. The analytical upper bound is found to be tight at moderate to high SNRs. Also, the proposed RPM-LM is found to perform

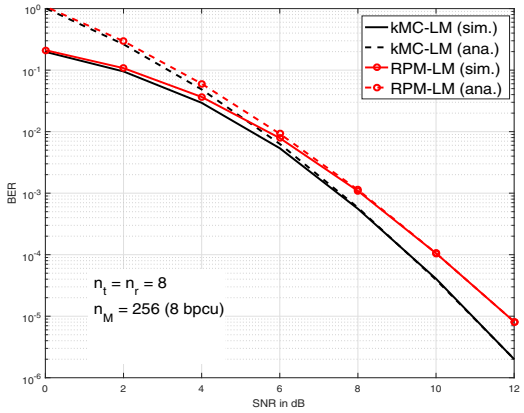

Fig. 2. BER performance of RPM-LM and kMC-LM with $n_t = n_r = 8$, $n_M = 256$ (8 bpcu), and ML detection. Analysis and simulation.

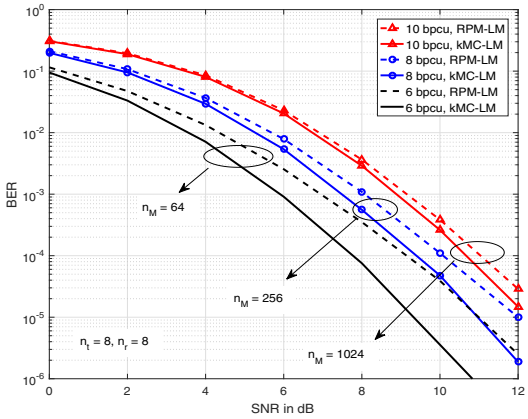

Fig. 4. BER performance of RPM-LM and kMC-LM for $n_t = n_r = 8$, $n_M = 64, 256, 1024$ (6,8,10 bpcu), and ML detection.

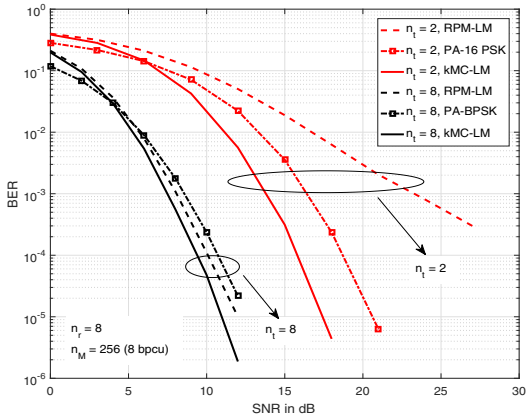

Fig. 3. BER performance of RPM-LM, kMC-LM, and PA-PSK for different n_t $(= 2, 4, 8)$ with $n_r = 8$, $n_M = 256$ (8 bpcu), and ML detection.

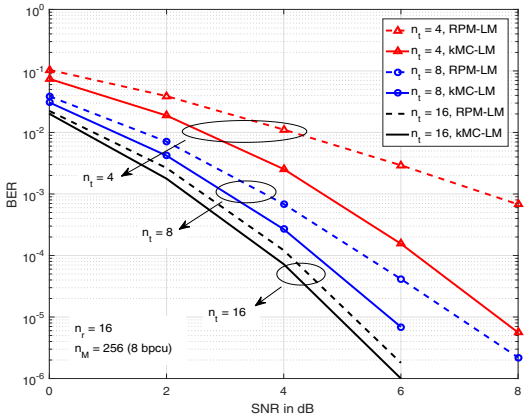

Fig. 5. BER performance of RPM-LM and kMC-LM for $n_t = 4, 8, 16$, $n_r = 16$, $n_M = 256$ (8 bpcu), and ML detection.

close to within a fraction of a dB (about 0.8 dB at 10^{-4} BER) compared to the performance of kMC-LM. Given their ease of generation, RPM-LM signal sets for large n_M, n_t are easily obtained; whereas generation of signal sets for large n_M, n_t using optimization algorithms such as kMC is complex.

Next, in Fig. 3, we show the effect of increasing the dimensionality of the signal set (i.e., varying n_t). We compare the performance of RPM-LM and kMC-LM for the following system parameters: $n_t = 2, 8$, $n_r = 8$, and $n_M = 256$ (8 bpcu). Note that, owing to their constant modulus nature, conventional PSK signal sets can be used as LM signal sets. Therefore, we present the performance of conventional PSK signal sets, which is called 'per-antenna PSK' (PA-PSK), as well for the same 8 bpcu (using 16-PSK and BPSK for $n_t = 2, 8$, respectively). The following observations can be made in Fig. 3.

- At a BER of 10^{-3}, kMC-LM performs better than PA-PSK by about 2.5 dB with $n_t = 2$ and by about 1 dB with $n_t = 8$. This better performance is because kMC-LM uses a signal set optimized jointly over the n_t dimensions, whereas PA-PSK repeats a per-dimension signal set over all the antennas.
- The performance of RPM-LM improves with increasing dimensionality (from $n_t = 2$ to 8) and gets increasingly close to kMC-LM performance. For example, at 10^{-3} BER, the performance of RPM-LM compared to kMC-LM performance improves from a gap of about 8 dB with $n_t = 2$ to about a fraction of a dB with $n_t = 8$.

In Fig. 4, we show the performance comparison between RPM-LM and kMC-LM for varying sizes of the signal sets, i.e., varying n_M, for $n_t = n_r = 8$. We show the performance for $n_M = 64, 256, 1024$, corresponding to 6,8,10 bpcu, respectively. We see that the performance gap between RPM-LM and kMC-LM decreases as the size of the signal set increases. For example, at a BER of 10^{-3}, the performance gap between RPM-LM and kMC-LM is about 1.5 dB for 6 bpcu ($n_M = 64$), and this gap reduces to about 0.4 dB for 10 bpcu ($n_M = 1024$).

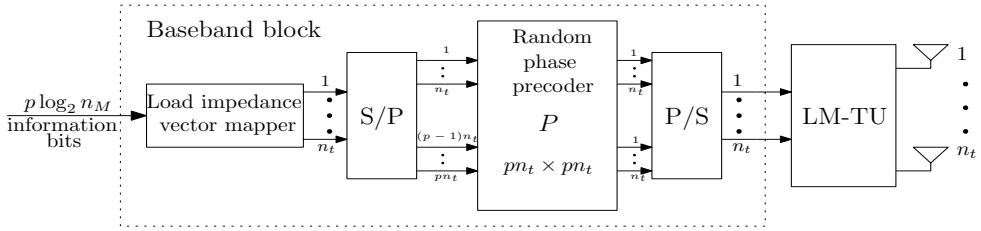

Fig. 7. LM transmitter with RPP.

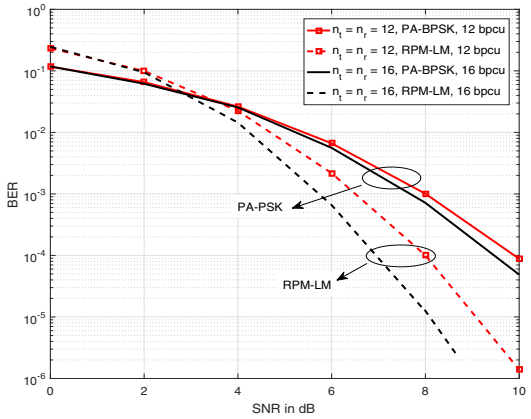

Fig. 6. BER performance of PA-PSK and RPM-LM for $n_t = n_r = 12, 16$, $n_M = 4096, 65536$ (12,16 bpcu), and ML detection.

Another performance comparison between RPM-LM and kMC-LM for varying $n_t (= 4, 8, 16)$ with $n_r = 16$, and $n_M = 256$ (8 bpcu) is shown in Fig. 5. As in Fig. 3, here again we see that the performance gap between RPM-LM and kMC-LM reduces for increasing dimensionality; for example, the performance gap reduces to just about 0.3 dB at 10^{-4} BER when the dimensionality is increased to $n_t = 16$.

In Fig. 6, we present the performance of RPM-LM for 12 and 16 bpcu, i.e., for $n_M = 4096$ and 65536, respectively. We note that generation of LM signal sets of such large sizes using kMC algorithm is prohibitively complex. So, in this case, we restrict our comparison only with PA-PSK. The following system parameters are considered; a) for 12 bpcu: $n_t = n_r = 12$ and $n_M = 4096$ for RPM-LM, and $n_t = n_r = 12$ and BPSK for PA-PSK, and b) for 16 bpcu: $n_t = n_r = 16$ and $n_M = 65536$ for RPM-LM, and $n_t = n_r = 16$ and BPSK for PA-PSK. We can see that, at 10^{-4} BER, RPM-LM performs better than PA-PSK by about 2 dB at 12 bpcu and by about 3 dB at 16 bpcu.

IV. RPP and PIM in LMAs

In this section, we propose the use of random phase precoding (RPP) [13],[14] and precoder index modulation (PIM) [18] in LMAs.

A. RPP in LMAs

RPP in LMAs is a technique where p LM signal vectors are precoded using a $pn_t \times pn_t$ precoder matrix consisting of random phases, and the resulting precoded vector is transmitted in p channel uses. By doing so, we provide time diversity opportunity that can be realized through joint signal detection over p channel uses. The LM signal set used can be generated using either RPM or optimization algorithms such as kMC.

Figure 7 shows the LM transmitter with RPP. It takes p LM signal vectors and concatenates them to form the $pn_t \times 1$ effective signal vector $\mathbf{x} \in \mathbb{S}_{\text{LM}}^p$, where $\mathbb{S}_{\text{LM}}$ is the LM signal set used. The vector $\mathbf{x}$ is then precoded using a $pn_t \times pn_t$ matrix $\mathbf{P}$ to get the transmit vector $\mathbf{Px}$. The (i,j)th entry of the precoder matrix $\mathbf{P}$ is $\frac{1}{\sqrt{pn_t}} e^{\mathbf{j}\theta_{i,j}}$, where $\mathbf{j} = \sqrt{-1}$ and the phases $\{\theta_{i,j}\}$ are generated using a pseudo-random sequence generator. The seed of this random number generator is shared a priori among the transmitter and receiver. The LM baseband block tunes the antenna loads according to the $\mathbf{Px}$ vector, the signals corresponding to which are transmitted by the LM-TU over p channel uses, resulting in a rate of $\log_2 n_M$ bpcu.

Let n_r denote the number of receive antennas. The $pn_r \times 1$ received signal vector at the end of p channel uses is

$$\mathbf{y} = \mathbf{DPx} + \mathbf{n}, \tag{11}$$

where $\mathbf{D} = \text{diag}\{\mathbf{H}_{(1)} \ \mathbf{H}_{(2)} \cdots \mathbf{H}_{(p)}\}$, $\mathbf{H}_{(i)}$ is the $n_r \times n_t$ channel matrix in the ith channel use, the elements of $\mathbf{H}_{(i)}$ are assumed to be i.i.d. $\mathcal{CN}(0,1)$, and $\mathbf{n}$ is the $pn_r \times 1$ noise vector $[\mathbf{n}_{(1)}^T \mathbf{n}_{(2)}^T \cdots \mathbf{n}_{(p)}^T]^T$, where the entries of the $n_r \times 1$ noise vector in the ith channel use $\mathbf{n}_{(i)}$ are distributed as $\mathcal{CN}(0, \sigma^2)$. We note that $\|\mathbf{DP}\|_F = \|\mathbf{D}\|_F$. This creates a $pn_r \times pn_t$ virtual MIMO system, providing a p-fold increase in dimensions in time and a resulting opportunity to obtain time diversity gain. The ML decision rule is given by

$$\hat{\mathbf{x}} = \underset{\mathbf{x} \in \mathbb{S}_{\text{LM}}^p}{\text{argmin}} \|\mathbf{y} - \mathbf{DPx}\|^2. \tag{12}$$

Simulation results: In Fig. 8, we present the BER performance of kMC-LM with RPP for $n_t = n_r = 2$, $n_M = 16$ (4 bpcu), and ML detection. We present the BER plots for $p = 2, 4$. For comparison purposes, we also present the performance of kMC-LM without RPP. From Fig. 8, we see that kMC-LM with RPP performs better than kMC-LM without RPP by about 3 dB for $p = 2$ at 10^{-4} BER, and the performance improvement

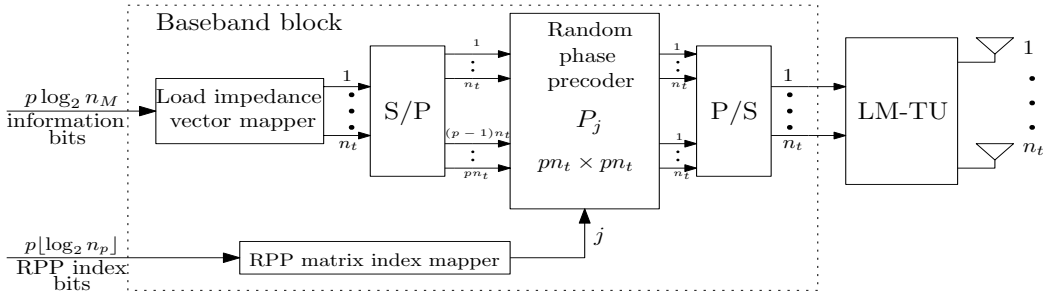

Fig. 9. LM transmitter with PIM.

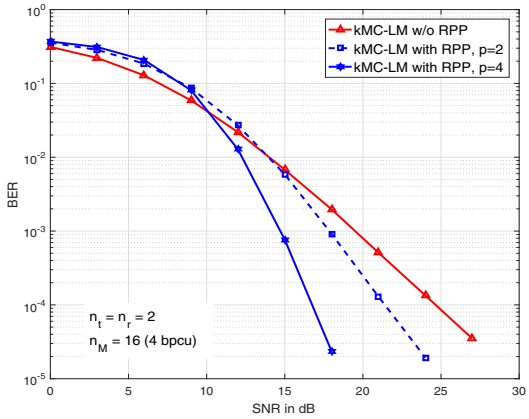

Fig. 8. BER performance of RPP-LM with $p = 2, 4$ and kMC-LM for $n_t = n_r = 2$, $n_M = 16$ (4 bpcu), and ML detection.

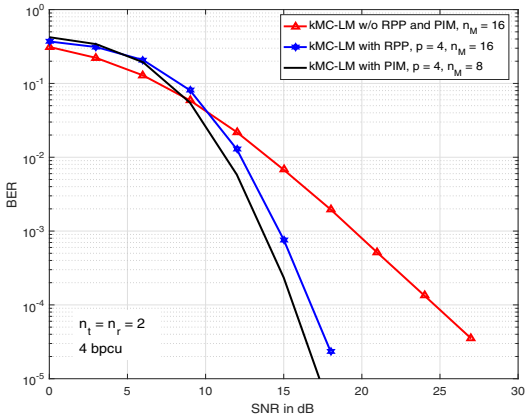

Fig. 10. BER performance of three schemes with $n_t = n_r = 2$, 4 bpcu, and ML detection: i) kMC-LM without RPP and PIM, $n_M = 16$, ii) kMC-LM with RPP, $p = 4$, $n_M = 16$, and iii) kMC-LM with PIM, $p = 4$, $n_M = 8$.

increases to about 8 dB for $p = 4$. This improvement in performance is because of the time diversity advantage that RPP offers.

B. PIM in LMAs

In index modulation schemes, information bits are conveyed through the choice of transmit entities such as transmit antennas, subcarriers, and precoders which get activated during data transmission [15]-[18]. Index modulation schemes offer the benefits of hardware simplicity and good performance. In this subsection, we study the use of PIM in LMAs. When PIM is used in LMAs, information bits are conveyed through the choice (index) of a precoder matrix among a set of predetermined precoder matrices, in addition to conveying information bits through the LM signal vectors. The LM transmitter with PIM is shown in Fig. 9.

Denote a collection of $pn_t \times pn_t$ precoder matrices as $\mathbb{P} = \{\mathbf{P}_1, \mathbf{P}_2, \cdots, \mathbf{P}_{|\mathbb{P}|}\}$, where $|\mathbb{P}|$ denotes the cardinality of the set $\mathbb{P}$. Each precoder matrix in $\mathbb{P}$ is taken to be a RPP matrix generated as in the previous subsection (Sec. IV-A). One of these matrices is chosen to precode p LM signal vectors in p channel uses. The choice of which of the $|\mathbb{P}|$ precoder matrices is used is made using $\lfloor\log_2 |\mathbb{P}|\rfloor$ information bits - called the RPP index bits. This is in addition to $p\log_2 n_M$ bits conveyed by p LM signal vectors. Therefore, the achieved rate in LM with PIM is given by $\frac{1}{p}\big(\lfloor\log_2 |\mathbb{P}|\rfloor + p\log_2 n_M\big)$ bpcu. Note that the achieved rate in LM without PIM is $\log_2 n_M$ bpcu. It can be seen that, to achieve the same bpcu as in LM without PIM, we need a smaller LM signal set size in LM with PIM, as additional bits are conveyed through the choice of RPP matrices. The $pn_r \times 1$ received signal vector in p channel uses is given by

$$\mathbf{y} = \mathbf{D}\mathbf{P}_j\mathbf{x} + \mathbf{n}, \tag{13}$$

where $\mathbf{P}_j$ is the RPP matrix chosen from $\mathbb{P}$, and $\mathbf{D}$, $\mathbf{x}$, and $\mathbf{n}$ are as described in the previous subsection (Sec. IV-A). The ML detection rule is given by

$$\{\hat{\mathbf{x}}, \hat{j}\} = \underset{\mathbf{x}\in\mathbb{S}_{\text{LM}}^p,\ j=1,\cdots,|\mathbb{P}|}{\operatorname{argmin}} \|\mathbf{y} - \mathbf{D}\mathbf{P}_j\mathbf{x}\|^2. \tag{14}$$

Simulation results: In Fig. 11, we present the BER performance of three schemes with $n_t = n_r = 2$, 4 bpcu, and ML detection. The schemes are: i) kMC-LM without RPP and PIM, $n_M = 16$, ii) kMC-LM with RPP, $p = 4$, $n_M = 16$, and iii) kMC-LM with PIM, $p = 4$, $n_M = 8$. Note that, in kMC-LM with PIM, 3 bpcu comes from LM signal vectors and 1 bpcu comes from RPP indexing. From Fig. 11, it is observed that, at 10^{-4} BER, kMC-LM with PIM performs better by

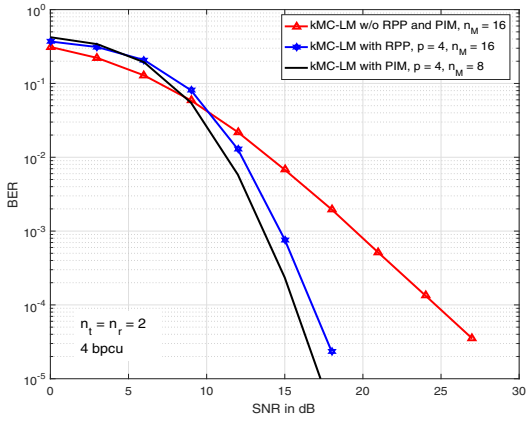

Fig. 11. BER performance of three schemes with $n_t = n_r = 2$, 4 bpcu, and ML detection: i) kMC-LM without RPP or PIM, $n_M = 16$, ii) kMC-LM with RPP, $p = 4$, $n_M = 16$, and iii) kMC-LM with PIM, $p = 4$, $n_M = 8$.

about 7-8 dB compared to kMC-LM with out RPP or PIM, and by about a dB compared to kMC-LM with RPP. This performance improvement is because of the smaller size of the signal set $(n_M = 8)$ used in kMC-LM with PIM compared to $n_M = 16$ used in the other two schemes; signal vectors in multidimensional hypersphere are better separated from each other in a smaller sized signal set compared to a larger set.

V. Conclusions

We proposed RPM as a simple and efficient way to generate signal sets for load modulated arrays, which is emerging as a promising transmitter architecture for MIMO systems. Load modulated arrays are attractive because of their RF hardware simplicity. In RPM, randomly chosen phase vectors form the LM signal set. Because of its easy-to-generate advantage, RPM is attractive for the generation of LM signal sets of large size and dimensionality, where generation using optimization algorithms such as k-means clustering becomes prohibitively complex. The LM signal sets generated by RPM were shown to achieve good performance as well; for example, the signal sets generated using RPM were shown to perform close to the performance of the signal sets constructed using kMC algorithm within fraction of a dB when the signal set size and dimensionality are large. We also demonstrated that, because of their time diversity and indexing advantages, RPP and PIM improved the performance of LM schemes.

References

[1] D. Tse and P. Viswanath, *Fundamentals of Wireless Communication*, Cambridge Univ. Press, 2005.

[2] A. Goldsmith, *Wireless Communications*, Cambridge Univ. Press, 2005.

[3] A. Chockalingam and B. S. Rajan, *Large MIMO Systems*, Cambridge Univ. Press, Feb. 2014.

[4] E. G. Larsson, F. Tufvesson, O. Edfors, and T. L. Marzetta, "Massive MIMO for next generation wireless systems," *IEEE Commun. Mag.*, vol. 52, no. 2, pp. 186-195, Feb. 2014.

[5] Z. Hasan, H. Boostanimehr, and V. K. Bhargava, "Green cellular networks: a survey, some research issues and challenges," *IEEE Commun. Surveys & Tutorials*, vol. 13, no. 4, pp. 524-540, 4th quarter, 2011.

[6] M. A. Sedaghat, V. I. Barousis, R. R. Müller, and C. B. Papadias, "Load modulated arrays: a low-complexity antenna," *IEEE Commun. Mag.*, vol. 54, no. 3, pp. 46-52, Mar. 2016.

[7] R. R. Müller, M. A. Sedaghat, and G. Fischer, "Load modulated massive MIMO," *Proc. IEEE GlobalSIP'2014*, pp. 622-626, Dec. 2014.

[8] C. Rachinger, R. R. Müller, and J. B. Huber, "Phase-shift keying on the hypersphere: power-efficient MIMO communications," online: arXiv:1611.01009v3[cs.IT] 20 Dec 2016.

[9] M. A. Sedaghat, R. R. Müller, and C. Rachinger, "(Continuous) phase modulation on the hypersphere," *IEEE Trans. Wireless Commun.*, vol. 15, no. 8, pp. 5763-5774, Aug. 2016.

[10] N. J. A. Sloane. *Spherical Codes*, accessed in Apr. 2017. [Online]. Available: http://neilsloane.com/packings/

[11] I. S. Dhillon and D. S. Modha, "Concept decompositions for large sparse text data using clustering," *Machine Learning*, vol. 42, no. 1, pp. 143-175, Jan. 2001.

[12] M. S. Alouini and A. Goldsmith, "A unified approach for calculating error rates of linearly modulated signals over generalized fading channels," *IEEE Trans. Commun.*, vol. 47, no. 9, pp. 1324-1334, Sep. 1999.

[13] R. Annavajjala and P. V. Orlik, "Achieving near exponential diversity on uncoded low-dimensional MIMO, multi-user and multi-carrier systems without transmitter CSI," *Proc. ITA'2011*, Jan. 2011.

[14] T. L. Narasimhan, Y. Naresh, T. Datta, and A. Chockalingam, "Pseudo-random phase precoded spatial modulation and precoder index modulation," *Proc. IEEE GLOBECOM'2014*, pp. 3868-3873, Nov. 2014.

[15] E. Basar, "Index modulation techniques for 5G wireless networks," *IEEE Commun. Mag.*, vol. 54, no. 7, pp.168-175, Jul. 2016.

[16] E. Basar, U. Aygolu, E. Panayirci, and H. V. Poor, "Orthogonal frequency division multiplexing with index modulation," *IEEE Trans. Signal Process.*, vol. 61, no. 22, pp. 5536-5549, Nov. 2013.

[17] T. Datta, H. Eshwaraiah, and A. Chockalingam, "Generalized space-and-frequency index modulation," *IEEE Trans. Veh. Tech.*, vol. 65, no. 7, pp. 4911-4924, Jul. 2016.

[18] Y. Naresh, T. Lakshmi Narasimhan, and A. Chockalingam, "Capacity bounds and performance of precoder index modulation," *Proc. IEEE WCNC'2016*, Apr. 2016.